# Optical functions of uniaxial ZnO determined by generalized ellipsometry

G. E. Jellison, Jr. and L. A. Boatner
*Solid State Division, Oak Ridge National Laboratory, Oak Ridge, Tennessee 37831-6030*
(Received 2 February 1998; revised manuscript received 9 April 1998)

The optical functions of uniaxial ZnO have been determined using two-modulator generalized ellipsometry, where a single measurement is sufficient to determine the optical functions from appropriately aligned uniaxial crystals. Above the direct band edge ($\sim$3.3 eV), this technique produces the most accurate values of the optical functions of ZnO presently available, while the refractive indices determined below the direct band edge agree with minimum-deviation methods. Near the direct band edge, the optical functions are modified by the excitonic interaction with a three-dimensional critical point. The optical dielectric response functions are fit to a recent formulation by Holden *et al.* [Phys. Rev. B **56**, 4037 (1997)]. One isotropic point in the spectrum was observed at 3.114 eV, and a near-isotropic point near 3.31–3.34 eV. [S0163-1829(98)05428-9]

Zinc oxide (ZnO) is an $n$-type direct-gap semiconductor with a wurtzite crystal structure. Optically, ZnO is uniaxial, defined by a dielectric function for light polarized parallel to the $c$ axis ($E\|c$ or extraordinary), and a dielectric function for light polarized perpendicular to the $c$ axis ($E\perp c$ or ordinary). The band gap of the material is large ($\sim$3.3 eV), making it of considerable technological interest for both electrical and optical applications. Recently, room-temperature optically pumped lasing has been observed in thin films of ZnO grown by plasma-enhanced molecular-beam epitaxy on sapphire.[1]

In the early 1960s, several workers reported the results of optical reflection studies of ZnO that showed the presence of an exitonic structure in the optical spectra near the direct band edge. These early studies[2] measured the optical reflection for light polarized parallel and perpendicular to the $c$ axis, and used Kramers-Kronig analysis to determine the optical functions. Later, workers prepared very thin samples of ZnO and measured the optical transmission through the material for light polarized with either $E\|c$ or $E\perp c$.[3,4] For light below the direct band edge, traditional angle-of-minimum-deviation methods produced very accurate values of the refractive index for both $E\|c$ and $E\perp c$.[5] Freeouf[6] obtained much better values of the dielectric functions by measuring the reflectivity from 0.6 to 20–30 eV before applying the Kramers-Kronig analysis to determine the dielectric functions. Matz and Lütz[7] determined the optical functions of ZnO using nulling ellipsometry at several wavelengths defined by interference filters. Very recently, Hu *et al.*[8] used optical transmission to measure the optical functions of thin-film ZnO prepared by pulsed-laser deposition.

In this Brief Report, we describe the procedure used to determine the anisotropic optical functions of ZnO using two-modulator generalized ellipsometry (2-MGE).[9,10] We will show that the optical functions for ZnO determined using 2-MGE are the most accurate available in the region from the band gap to the measurement limits of the instrument (i.e., $\sim$3.3–5 eV). In addition, the optical functions obtained below the band edge (1.45 to $\sim$2.8 eV) agree with minimum deviation measurements,[5] within the limits of error.

The 2-MGE is described in detail in Refs. 9 and 10, and the analysis technique used to determine the optical functions for uniaxial materials from 2-MGE measurements is described in Ref. 11 for rutile ($TiO_2$). Briefly, 2-MGE uses two photoelastic modulator-polarizer pairs, one in the polarization-state generator (PSG) arm of the ellipsometer and the other in the polarization-state detector (PSD) arm. Each modulator operates at a different resonant frequency (50.2 and 60.2 kHz in our case), making it possible to measure eight different elements of the reduced sample Mueller matrix. If the PSG and PSD are aligned at (0, |45|) or (|45|, 0) with respect to the plane of incidence, then it is possible to determine completely the light reflection from a nondepolarizing sample. That is, the entire reduced Jones matrix of the sample

$$\mathbf{J}=\begin{pmatrix} \rho_{pp} & \rho_{ps} \\ \rho_{sp} & 1 \end{pmatrix} \tag{1}$$

can be determined with a single measurement. In Eq. (1), $\rho_{pp}=r_{pp}/r_{ss}$, $\rho_{ps}=r_{ps}/r_{ss}$, and $\rho_{sp}=r_{sp}/r_{ss}$, where $r_{pp}$ and $r_{ss}$ are the complex reflection coefficients for $p$- and $s$-polarized light, respectively, and $r_{sp}$ and $r_{ps}$ are the cross-polarization complex reflection coefficients.

Since the features of the optical spectrum of ZnO are very narrow near the band edge, it was essential to improve the wavelength resolution of the monochromator described in Ref. 9. This was done by replacing the untapered optical fiber (400-$\mu$m diameter) with a 400–200-$\mu$m tapered fiber coupled directly to the monochromator (thus eliminating the $f$/# matcher), making the input slit the exit aperture of the tapered fiber (200 $\mu$m). The resulting resolution of this configuration was measured using the light from a HeNe laser, and was found to be 0.5 nm when the exit slit of the monochromator was set to 100 $\mu$m or less. The measurement requires only that the optical axis of the sample be significantly off-normal to avoid zeros in the off-diagonal elements $\rho_{sp}$ and $\rho_{ps}$ caused by symmetry.[11] If this is satisfied, then it is possible to determine the complex dielectric functions $\varepsilon_{1o}(E)$, $\varepsilon_{1e}(E)$, $\varepsilon_{2o}(E)$, and $\varepsilon_{2e}(E)$ with a single measurement. [Here the subscript $o$ means ordinary, ($E\perp c$); and $e$ means extraordinary, ($E\|c$).]

 

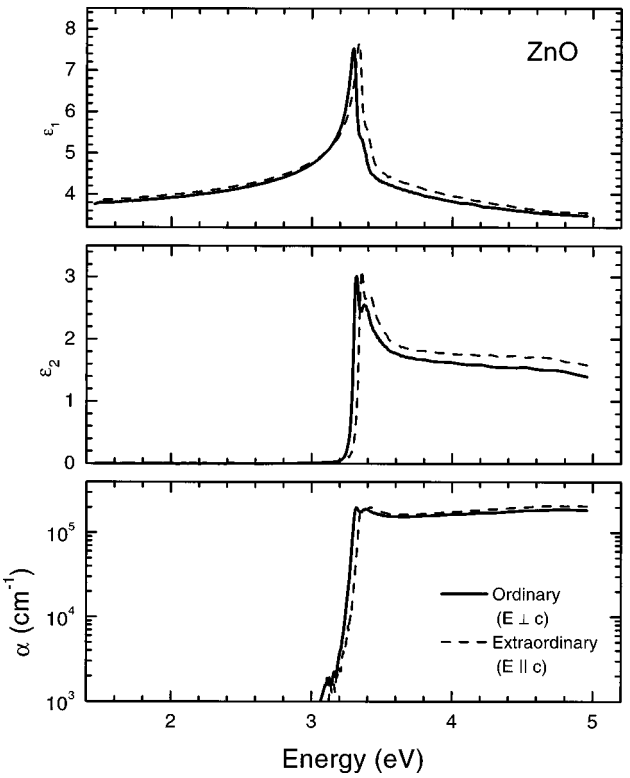


FIG. 1. The real and imaginary parts of the complex dielectric function ($\varepsilon_1$ and $\varepsilon_2$) and the absorption coefficient ($\alpha$) of ZnO grown by vapor transport and measured at room temperature.

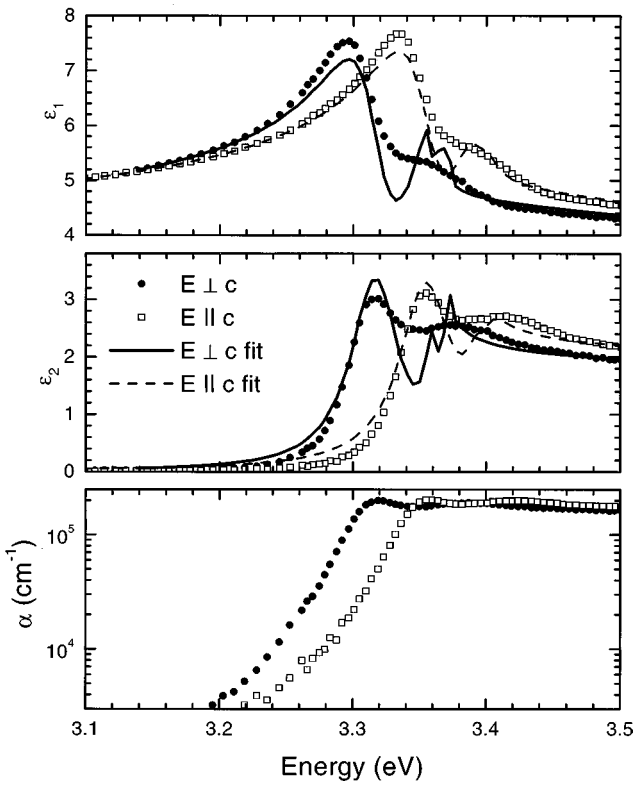


FIG. 2. The same data set as Fig. 1, but over the 3.1–3.5-eV range. The solid and dashed lines indicate fits to the data using Eq. (2).

Three different samples of ZnO were measured using 2-MGE. One sample was grown using the chemical vapor transport method (denoted as sample VT), and another by the hydrothermal method by Airtron Industries (denoted as sample *H*). In order to examine the effect of doping on the exitonic structures, a vapor-transport-grown ZnO sample doped with Sn was also measured using 2-MGE. The VT and *H* samples were clear, while the Sn-doped VT sample was black. The optic axes of the VT and *H* samples were in the plane of the sample surface ($\theta \sim 90°$), while the optic axis of the doped sample was $59° \pm 2°$ off-normal as measured by x-ray analysis. All measurements were performed at room temperature.

Below the band edge ($\sim 3.3$ eV), undoped ZnO is transparent, implying that $\varepsilon_2$ ($E < 3$ eV) $< 10^{-5}$. Therefore, the fact that $\mathrm{Im}(\rho_{pp}) > 0$ indicates the presence of a surface overlayer. To correct for this overlayer, the 2-MGE data from 1.46 to $\sim 3.1$ eV were fit to a three-medium model, consisting of air/surface roughness/ZnO, where the surface roughness was modeled using a 50% air, 50% ZnO Bruggeman effective medium, and the transparent ZnO was modeled using a traditional Lorentz approximation for both $n_o(E)$ and $n_e(E)$. The overlayer thickness and directions of the optical axes were treated as fitting parameters, which were then used to determine the optical functions of ZnO as described in Ref. 11, including error limits. The results are shown in Figs. 1 and 2 for the VT sample. Near and above the critical points ($\sim 3.3$ eV) the resulting dielectric functions from the three samples were identical within error, while the refractive indices of the *H* and the Sn-doped VT samples were $\sim 0.012 \pm 0.007$ less than the refractive index of the undoped VT sample from 850 to $\sim 450$ nm.

The data for the refractive index at several wavelengths below the band edge are shown in Table I. For comparison, the data from Ref. 5 are included in Table I, where the refractive indices were obtained from prisms fabricated from vapor-transport-grown ZnO using the minimum-deviation method. While the 2-MGE approach is not as accurate as the minimum-deviation method below the direct band edge, the accuracy is still very good, and an accuracy of $\pm 0.003$ in $n_o(E)$ and $n_e(E)$ can be obtained. This technique gives similar values of the dielectric function for different samples, with different orientations of the optic axes, with different values of the surface roughness, and at different angles of incidence (60° and 65°).

No similar comparison can be made for the values of the dielectric function above the band edge. Well above 3.5 eV, the error limit of $\varepsilon_1$ and $\varepsilon_2$ was 0.03–0.05, while the error limit climbed to 0.10–0.15 in the 3.2–3.4-eV range. The dielectric functions determined by Kramers-Kronig integration of reflectance data of Freeouf[6] comes the closest, but the Kramers-Kronig technique is far more inaccurate than the ellipsometric technique, since it relies on more inaccurate data (reflectance) and requires extrapolations to perform the Kramers-Kronig integrals. Therefore, the 2-MGE technique is the most accurate technique available to determine the dielectric functions [$\varepsilon_{1o}(E)$, $\varepsilon_{1e}(E)$, $\varepsilon_{2o}(E)$, and $\varepsilon_{2e}(E)$] of uniaxial crystals above the band edge.

Two main features are observable in $\varepsilon_1$ and $\varepsilon_2$ near the direct band edge, and the $\varepsilon_{1e}$ and $\varepsilon_{2e}$ spectra are nearly the same shape as the $\varepsilon_{1o}$ and $\varepsilon_{2o}$ spectra—only shifted up in

TABLE I. A comparison of the refractive indices of ZnO below the band edge determined in this work and in Ref. 5. Both ZnO crystals were grown by the vapor transport method.

| Wavelength (nm) | Ordinary ($E\perp c$) | | | Extraordinary ($E\|c$) | | |
|---|---|---|---|---|---|---|
| | a | b | difference | a | b | difference |
| 450 | 2.1058[a] | 2.104[b] | 0.0018 | 2.1231[a] | 2.121[b] | 0.0021 |
| 500 | 2.0511[a] | 2.047[b] | 0.0041 | 2.0681[a] | 2.065[b] | 0.0031 |
| 600 | 1.9985[a] | 1.997[b] | 0.0015 | 2.0147[a] | 2.015[b] | −0.0003 |
| 700 | 1.9735[a] | 1.974[b] | −0.0005 | 1.9897[a] | 1.990[b] | −0.0003 |
| 800 | 1.9597[a] | 1.961[b] | −0.0013 | 1.9752[a] | 1.976[b] | −0.0008 |
| Error | 0.0001 | 0.003 | | 0.0001 | 0.003 | |

[a]Reference 5.
[b]This work.

energy and up in magnitude. From earlier work,[1–7] the two features can be identified as the $n=1$ and 2 excitons associated with a critical point in the joint density of states related to the one-electron band structure. Band-structure calculations of ZnO (Refs. 12–14) show that the conduction band (CB) near $\mathbf{k}=\mathbf{0}$ consists of a single band with very little anisotropy in the effective mass, and the top of the valence band (VB) consists of three bands, all of which contribute to near-edge absorption. From Ref. 3, the uppermost VB of wurtzite crystals is of $\Gamma_9$ symmetry, and optical transitions from this band to the $\Gamma_7$ CB are selection rule limited to $E\perp c$ transitions. Optical transitions from two other VB's ($\Gamma_7$ symmetry) are not selection rule limited, but the $E\|c$ transition is considerably stronger.[2] The $\varepsilon_{2e}$ spectrum is shifted up in energy compared to the $\varepsilon_{2o}$ spectrum by the energy difference between the $\Gamma_9$ VB and the top $\Gamma_7$ VB ($\sim 0.033$ eV). In addition, the $\varepsilon_{2e}$ spectrum is shifted up with respect to the $\varepsilon_{2o}$ spectrum, probably due to small differences in the average matrix element between the CB and the different VB's and to differences in the effective masses of the $\Gamma_9$ VB and the top $\Gamma_7$ VB. All of the VB's have considerably higher effective masses than does the CB. Noting the similar shape of the $\varepsilon_{2o}$ and $\varepsilon_{2e}$ spectra and ignoring the $\mathbf{k}$ dependence of the matrix elements, the shape of both the $\varepsilon_{2o}$ and $\varepsilon_{2e}$ spectra above $\sim 3.45$ eV is determined primarily by the density of states of the CB.

The presence of the excitons near the three-dimensional (3D) critical point modifies the dielectric function in this energy range.[15–20] Using a Lorentzian approximation for line-shape broadening of the excitonic states and the band edge, Holden *et al.*[19] determined that the dielectric function near a 3D critical point modified by excitonic interactions could be expressed using five parameters. After some algebraic manipulation of their Eqs. (A7)–(A10), this expression is given by

$$\varepsilon(E)=\frac{A}{2E^2}\left\{\sum_{n=1}^{\infty}\left[g_{b,n}(E+i\Gamma_n)-g_{b,n}(i\Gamma_n)\right]+g_u(E+i\Gamma_0)-g_u(i\Gamma_0)\right\}. \tag{2}$$

In Eq. (2),

$$g_{b,n}(\xi)=\frac{4R^2}{n^3}\left[\frac{1}{(E_o-\xi)^2-R^2/n^2}+\frac{1}{(E_o+\xi)^2-R^2/n^2}\right], \tag{3a}$$

$$g_u(\xi)=-\ln\left(\frac{E_o^2-\xi^2}{R^2}\right)-\frac{1}{2}\sum_{n=1}^{\infty}g_{b,n}(\xi)-\pi\left[\cot\left(\frac{\pi\sqrt{R}}{\sqrt{E_o-\xi}}\right)+\cot\left(\frac{\pi\sqrt{R}}{\sqrt{E_o+\xi}}\right)\right]. \tag{3b}$$

The five parameters are the amplitude $A$, the direct-band-gap energy $E_o$, the excitonic binding energy $R$, the broadening energy of the direct band gap $\Gamma_0$, and the broadening of the excitonic peak $\Gamma_0^{\mathrm{ex}}$. The broadening of the $n$th exciton peak is determined using the empirical relation[16]

$$\Gamma_n=\Gamma_0-\frac{\Gamma_0-\Gamma_0^{\mathrm{ex}}}{n^2}. \tag{3c}$$

Figure 2 shows the dielectric function spectra for ZnO near the 3.3-eV critical point determined from 2-MGE measurements, and the best fit to the data from Eq. (2). The results to the fit are tabulated in Table II, where an extra parameter $\varepsilon_1(\infty)$ is added to Eq. (2) to take into account transitions at higher energies [with no high-energy transitions, $\varepsilon_1(\infty)=1$]. The value $\chi^2$ listed in Table II is the reduced $\chi^2$ of the fit (taking into account the error limits of $\varepsilon_o$ and $\varepsilon_e$), and should be $\sim 1$ for a good fit of Eq. (2) to the data. Clearly, Eq. (2) fits the main features of the data, but

TABLE II. Parameters determined by fitting the dielectric functions of ZnO determined using 2-MGE to Eq. (2).

| | Ordinary ($E\perp c$) | Extraordinary ($E\|c$) |
|---|---|---|
| $E_o$ (eV) | 3.372±0.004 | 3.405±0.004 |
| $R$ (eV) | 0.056±0.002 | 0.050±0.003 |
| $\Gamma_0$ (eV) | 0.001±0.002 | 0.006±0.002 |
| $\Gamma_0^{\mathrm{ex}}$ (eV) | 0.023±0.002 | 0.024±0.002 |
| $A$ | 31.4±0.5 | 37.1±0.7 |
| $\varepsilon_1(\infty)$ | 2.66±0.03 | 2.52±0.03 |
| $\chi^2$ | 4.0 | 4.4 |

the high value of $\chi^2$ shows that the fit is not good. The difference between the data and the fit could come from a number of sources, including (1) the Lorentz approximation for broadening (which is known to give too much absorption below direct band edges), (2) the empirical expression for the broadening of the $n$th exciton [Eq. 3(c)], or (3) the parabolic and isotropic assumptions of the 3D critical point.

The fitted parameters shown in Table II indicate that the direct band edges of ZnO are 3.372 and 3.405 eV for the $E\perp c$ and $E\|c$ transitions, respectively, while the exciton binding energies are 0.056 and 0.050 eV, respectively. Low-temperature excitonic binding energies determined from transmission and reflection measurements were 0.059 eV (Ref. 2) and 0.061–0.067 eV.[4] The broadening of the excitons is 0.023–0.024 eV for both transitions, reminiscent of $kT$ broadening (0.026 eV at room temperature).

If it is assumed that $\varepsilon_{2o}=\varepsilon_{2e}=0$ below $\sim$3.15 eV, then there is an isotropic point for ZnO at $E=3.114$ eV, where $\varepsilon_{1o}=\varepsilon_{1e}=5.153$. Clearly this becomes a pseudoisotropic point if $\varepsilon_{2o}\neq\varepsilon_{2e}$ (or, equivalently, if the absorption coefficient $\alpha_o\neq\alpha_e$) at this energy. The 2-MGE is not sufficiently sensitive to measure $\alpha$ accurately for $\alpha<3\times10^3$ cm$^{-1}$. Since this is well below the lowest direct absorption edge, the primary absorption mechanisms are impurity absorption and $kT$ broadening of the $n=1$ excitonic peak. Therefore, a true isotropic point could be obtained with very pure crystals and at lower temperature. There also is a near-isotropic point near 3.3 eV (see the insets of Fig. 1), but this is not a true isotropic point, since $\varepsilon_{1o}=\varepsilon_{1e}=6.98$ at $E=3.308$, and $\varepsilon_{2o}=\varepsilon_{2e}=2.49$ at $E=3.341$.

While 2-MGE (as presently implemented in our laboratory) is not as sensitive as many reflectivity measurements in determining energies of transitions, nor is it as good as minimum deviation methods for measuring refractive indices in the *transparent* part of the spectrum, it is unparalleled in determining accurate values of the optical functions of uniaxial materials above the band edge. The 2-MGE can measure the entire reduced Jones matrix [Eq. (1)] in a single configuration. For orientations of the crystal where the off-diagonal elements ($\rho_{sp}$ and $\rho_{ps}$) are significantly different from zero, this one measurement is sufficient to determine $\varepsilon_{1o}(E)$, $\varepsilon_{1e}(E)$, $\varepsilon_{2o}(E)$, and $\varepsilon_{2e}(E)$ for uniaxial crystals. We have applied 2-MGE to a determination of the optical functions of ZnO and have shown that the spectra are easily explained by the presence of excitons near a 3D band edge. Additionally, an isotropic point exists at 3.114 eV, and a near-isotropic point near 3.31–3.34 eV.

The authors would like to acknowledge R. F. Wood for discussions of the excitonic structure and for carefully reading this manuscript. This research was sponsored by the Division of Material Science, U.S. Department of Energy under Contract No. DE-AC05-96OR22464 with Lockheed Martin Energy Research Corp.

[1] D. M. Bagnall, Y. F. Chen, Z. Zhu, T. Yao, S. Koyama, M. Y. Shen, and T. Goto, Appl. Phys. Lett. **70**, 2230 (1997).
[2] D. G. Thomas, J. Phys. Chem. Solids **15**, 86 (1960).
[3] B. Segall, Phys. Rev. **163**, 769 (1967).
[4] W. Y. Liang and A. D. Yoffe, Phys. Rev. Lett. **20**, 59 (1968).
[5] W. L. Bond, J. Appl. Phys. **36**, 1674 (1965).
[6] J. L. Freeouf, Phys. Rev. B **7**, 3810 (1973).
[7] R. Matz and H. Lütz, Appl. Phys. **18**, 123 (1979).
[8] W. S. Hu, Z. G. Liu, J. Sun, S. N. Zhu, Q. Q. Xu, D. Feng, and Z. M. Ji, J. Phys. Chem. Solids **58**, 853 (1997).
[9] G. E. Jellison, Jr. and F. A. Modine, Appl. Opt. **36**, 8184 (1997).
[10] G. E. Jellison, Jr. and F. A. Modine, Appl. Opt. **36**, 8190 (1997).
[11] G. E. Jellison, Jr., F. A. Modine, and L. A. Boatner, Opt. Lett. **22**, 1808 (1997).
[12] M. Cardona, J. Phys. Chem. Solids **24**, 1543 (1963).
[13] J. R. Cheilikowsky, Solid State Commun. **22**, 351 (1977).
[14] Y.-N. Xu and W. Y. Ching, Phys. Rev. B **48**, 4335 (1993).
[15] R. J. Elliott, Phys. Rev. **108**, 1384 (1957).
[16] R. Le Toullec, N. Piccioli, and J. C. Chevin, Phys. Rev. B **22**, 6162 (1980).
[17] A. Goñi, A. Canterero, K. Syassen, and M. Cardona, Phys. Rev. B **41**, 10 111 (1990).
[18] C. Tanguy, Phys. Rev. Lett. **75**, 4090 (1995).
[19] T. Holden, P. Ram, F. H. Pollak, J. L. Freeouf, B. X. Yang, and M. C. Tamargo, Phys. Rev. B **56**, 4037 (1997).
[20] P. Yu and M. Cardona, *Fundamentals of Semiconductors* (Springer-Verlag, New York, 1996).